18. LIMITED EVIDENCE OF ANTHROPOGENIC INFLUENCE ON THE 2011–12 EXTREME RAINFALL OVER SOUTHEAST AUSTRALIA

Andrew D. King, Sophie C. Lewis, Sarah E. Perkins, Lisa V. Alexander, Markus G. Donat, David J. Karoly, and Mitchell T. Black

Introduction. The 2010–12 period was characterized by well-above-average rainfall over much of Australia. The wetter conditions brought an end to the 13-year drought in southeastern (SE) Australia, although they also led to severe flooding across large areas of New South Wales and Victoria in early 2012. Both total and extreme rainfall were above average in the austral warm seasons (October–March) of 2010–11 and 2011–12 across SE Australia [2011–12 spatial anomalies are shown in Figs. 18.1a and 18.1b for rainfall totals and maximum consecutive five-day rainfall (Rx5day; Zhang et al. 2011) respectively]. Many stations across this region broke daily and multiday rainfall records as well as monthly records during February and March 2012 (Bureau of Meteorology 2012; Ganter and Tobin 2013).

ENSO is the primary driver of climate variability in eastern Australia (Nicholls et al. 1997) with greater rainfall totals during La Niña seasons than El Niño seasons in SE Australia (Fig. 18.1c). There is an asym-

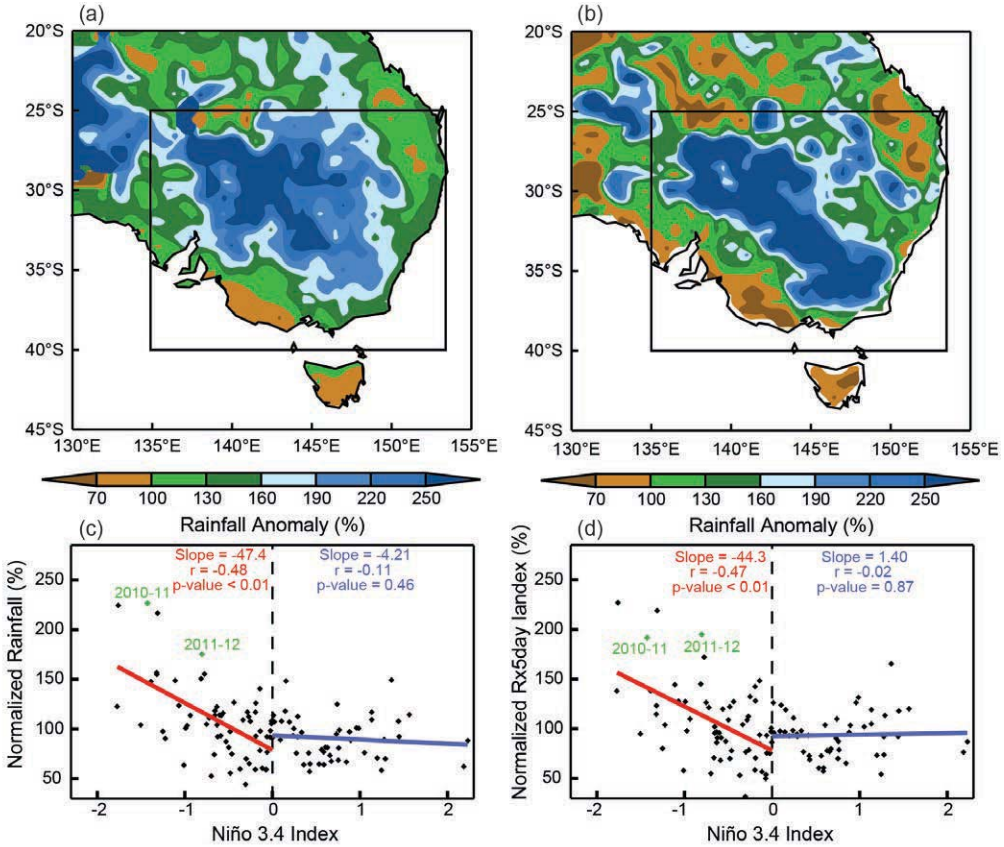

Fig. 18.1. Maps of Oct 2011–Mar 2012 (a) total rainfall and (b) Rx5day anomalies as a percentage of the Oct–Mar mean seasonal rainfall and Rx5day, respectively, for the period 1900–2012. The boxed region represents our area of study. Scatter plots of Oct–Mar Niño-3.4 SSTAs against area-averaged Oct–Mar (c) total rainfall and (d) Rx5day values for southeast Australia. Lines of best fit, calculated using ordinary least squares regression, are shown for warm SSTA (red) and cool SSTA (blue) seasons with corresponding slope values. The correlation (Spearman's Rank, r) and the significance of the fit (p-value) are also shown. The recent 2010-11 and 2011-12 seasons are marked in green.

metry whereby negative SST anomalies have a greater effect than positive SST anomalies on rainfall totals. Similar asymmetric relationships were reported by Power et al. (2006) for the Australian continent as a whole and by Cai et al. (2010) for SE Queensland.

A strong asymmetric ENSO-extreme rainfall teleconnection also exists for the SE Australia region (Fig. 18.1d) for area-averaged values of Rx5day. King et al. (2013) observed an asymmetric ENSO-extreme rainfall relationship for eastern Australia. The 2010–11 and 2011–12 seasons are two of the four largest Rx5day totals in the 1900–2012 series. This begs the question whether anthropogenic effects on the climate have affected the ENSO-extreme rainfall relationship, thus altering the probability of extreme rainfall in this area.

Data and methods. Observed monthly total rainfall and Rx5day amounts were calculated from the Australian Water Availability Project (AWAP) gridded dataset of daily rainfall (Jones et al. 2009) interpolated onto a regular 0.5° grid. Anomalies from the 1900–2012 means of total rainfall and Rx5day were calculated for each grid box separately. SSTs in the Niño-3.4 region (5°N–5°S, 170°W–120°W) were used as an index for ENSO from the HadISST dataset (Rayner et al. 2003). Observed total and Rx5day anomalies were averaged across the SE Australia region as defined by the boxed area (25°S–40°S, 135°E–154°E) in Fig. 181a,b and plotted against Niño-3.4 SSTs (Fig. 18.1c,d). As Rx5day anomalies at individual gridboxes were calculated relative to the gridbox mean values, the area-average Rx5day values are not biased towards wetter areas of SE Australia. The boxed region includes Australia's largest cities (i.e., Sydney, Melbourne, and Brisbane), with more than three-quarters of the country's population, and the entire Murray-Darling Basin, an area accounting for over 40% of Australia's agricultural production in terms of gross value (Nicholls 2004).

To make inferences about potential anthropogenic impacts, historical runs from models in the Coupled Model Intercomparison Project phase 5 (CMIP5) archive (Taylor et al. 2012) were analyzed and compared with observations. Ten models were selected based on the availability of data in the Australian node of the CMIP5 data repository and on their ability to capture variability in ENSO (see Supplementary Table S18.1). As ENSO strongly drives Australian rainfall variability, models that do not capture ENSO variability cannot replicate the observed teleconnection. These ten models adequately capture the amplitude of variability in Niño-3.4 region surface air temperatures seen in the observational HadCRUT4 dataset (Morice et al. 2012). The absolute SE Australia Rx5day amounts were taken from data downloaded from Environment Canada's CLIMDEX website (http://www.cccma.ec.gc.ca/data/climdex/; Sillmann et al. 2013). Rx5day anomalies were first calculated for each grid box in each model run and then averaged over the SE Australia domain. The anomalies were calculated in the same way as for the observations, so the area-averaged Rx5day anomaly values are not biased towards wetter areas. Sea surface temperature anomalies (SSTAs) in the Niño-3.4 region and Rx5day anomaly values for SE Australia were calculated for each individual model run and examined against each other per model. All models had greater Rx5day values in La Niña seasons than El Niño seasons. Models that did not have a stronger relationship between Niño-3.4 SSTAs and Rx5day when SSTAs are negative than when they are positive were removed leaving five models to be analyzed in more detail (models in bold in Supplementary Table S18.1). The area-averaged Rx5day anomaly values for each model were normalized against the model mean values over the historical period. Niño-3.4 SSTAs and normalized values of Rx5day could then be plotted together for the five models studied.

To examine for possible changes in extreme rainfall and in the ENSO-extreme rainfall teleconnection, the relationships in the modeled 1861–90 and 1976–2005 periods were compared. The earlier period (1861–90) was used to represent a time of much lower anthropogenic influence on the climate than the later period. Values of Rx5day in La Niña seasons only (defined as October–March seasons with SSTAs less than -0.5°C) were used to plot probability distribution functions (PDFs) in the two 30-year periods and these were examined for anthropogenic signals. Any low-frequency variability in the model runs would be unlikely to influence our results as multiple model runs were considered together. To examine the effect of ENSO variability, PDFs of La Niña Rx5day values and all other seasons' values through the entire historical period were also analyzed.

A Kolmogorov-Smirnov (KS) test was used to quantify differences between the respective sets of PDFs. Each PDF was bootstrapped 1000 times based on sub-samples of 50% of the smaller data sample being examined. Fractional Attributable Risk (FAR; Allen 2003) was calculated to examine change in risk of extreme rainfall events associated with anthropogenic influences and ENSO variability. FAR was

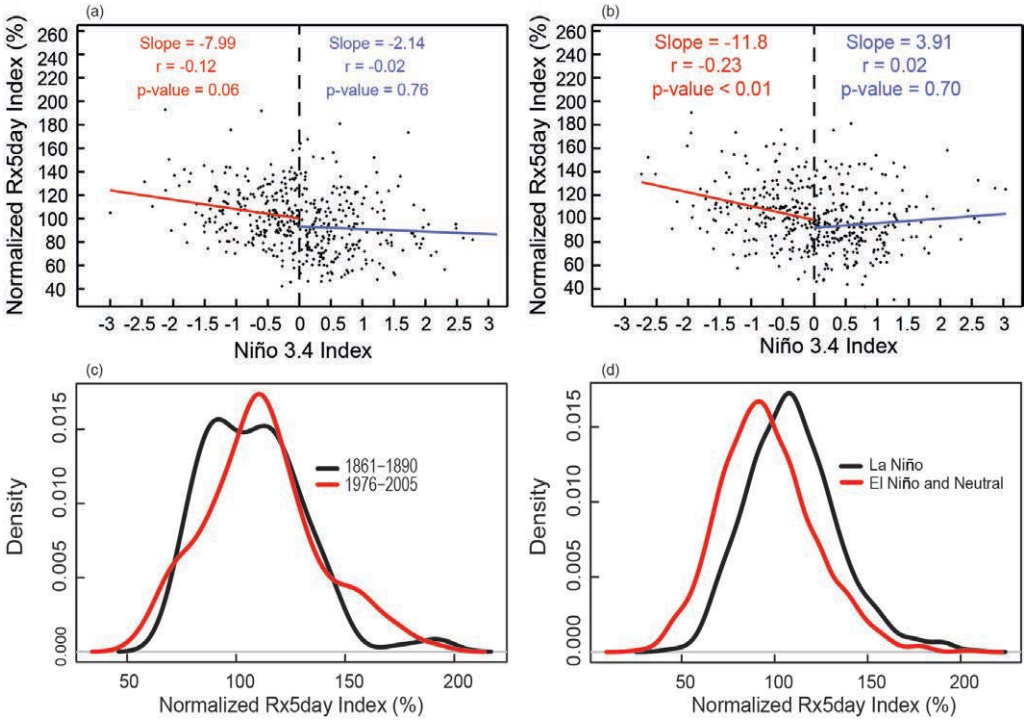

Fig. 18.2. (a) and (b) Scatter plots of Oct–Mar Niño-3.4 SSTAs against area-averaged Oct–Mar Rx5day values for southeast Australia for five CMIP5 models. Lines of best fit, calculated using ordinary least squares regression, are shown for warm SSTA (red) and cool SSTA (blue) seasons with corresponding slope values. The correlation (Spearman's Rank, r) and the significance of the fit (p-value) are also shown. These scatter plots are for the (a) 1861–90 and (b) 1976–2005 periods. PDFs of (c) La Niña-only normalized Rx5day values in the 1861–90 (black line) and 1976–2005 (red line) periods from the five CMIP5 models and of (d) La Niña-only (black line) and El Niño and Neutral (red line) normalized Rx5day values for the entire historical period from the five CMIP5 models.

calculated using Rx5day values above 150% of the mean Rx5day over the entire period to compare the frequency of extreme events between the early and late periods, and La Niña and all other events. The 150% threshold permitted the inclusion of only extreme rainfall events and provided a reasonable sample size for the FAR calculation.

All analysis involving both observations and models was done over October–March periods, coinciding with the peak in the annual ENSO cycle and the warm season in SE Australia when more of the extreme rainfall events occur.

Results. The analysis was conducted using the subselection of five CMIP5 models (those in bold in Supplementary Table S18.1), as the relationship in La Niña seasons is reproduced to some degree. The ENSO-extreme rainfall relationship is plotted for all five models combined, for the 1861–90 and 1976–2005 periods (Figs. 18.2a,b). There is little obvious change in the relationship between the two periods. On average, Rx5day values are 1.9% greater in the latter period than the earlier one. The increase is slightly weaker in La Niña seasons (1.3%) than El Niño (October–March with SSTAs greater than 0.5°C) seasons (3.4%).

The normalized Rx5day values in La Niña seasons only were selected to form PDFs for each of the 30-year periods (Fig. 18.2c). These PDFs are based on 124 samples for the 1861–90 period and a sample size of 119 for 1976–2005. There is some difference between the two PDFs in terms of their shape, but a KS-test suggests the two PDFs are not significantly different (at the 5% level). Examining values above a 150% threshold in the two periods gives a FAR value of +64% (with a standard deviation of ±22% calculated through bootstrapping) for extreme Rx5day values due to anthropogenic climate change in the recent period. It is worth noting that the FAR value is strongly sensitive to choice of threshold, selection of models, and region of study. Therefore, a robust anthropogenic influence cannot be detected.

Taking all normalized Rx5day values across the historical period in La Niña seasons and comparing with those values from neutral and El Niño seasons,

the PDFs shown in Fig. 18.2d were plotted. These PDFs are formed from 637 samples representing La Niña Rx5day values and 1523 samples representing El Niño and neutral Rx5day values. These PDFs are significantly different. FAR values show an increase in the likelihood of Rx5day values above a 150% threshold of 58% (with a standard deviation of ±15% across the 1000 estimates) in La Niña seasons compared with El Niño and neutral seasons combined. This FAR value is robust to the choice of threshold used.

Conclusions. We examined SE Australia extreme rainfall and its teleconnection with ENSO in observations and a selection of CMIP5 models. In observations, the magnitude of anomalously cool SSTs in the Niño-3.4 region has a far greater effect on Rx5day in SE Australia compared to the magnitude of anomalously warm SSTs. Five CMIP5 models were selected as the focus for our study as they possess aspects of ENSO variability and an asymmetric ENSO-extreme rainfall relationship. Using these models, we found little evidence of significant change in the ENSO-extreme rainfall relationship between 1861–90 and 1976–2005. The PDFs of Rx5day values in La Niña seasons also show nonsignificant differences between the same periods. There is little robust change in the risk of extreme rainfall events between 1861–90 and 1976–2005. Interannual variability related to ENSO has played a greater role than any long-term trend on the magnitude of extreme rainfall events in southeast Australia over the period 1861–2005. In summary, we detect limited evidence of a change in the relationship between ENSO and SE Australia extreme rainfall, or of a change in extreme rainfall itself, that may be attributed to anthropogenic climate change. Similar analysis of the austral summer mean rainfall anomalies in 2010–11 and 2011–12 also show some influence from La Niña with no apparent influence from anthropogenic climate change in the observed rainfall anomalies.

19. AN ATTRIBUTION STUDY OF THE HEAVY RAINFALL OVER EASTERN AUSTRALIA IN MARCH 2012

Nikolaos Christidis, Peter A. Stott, David J. Karoly, and Andrew Ciavarella

Introduction. Heavy rains at the end of summer 2012 across eastern Australia (Bureau of Meteorology 2012) led to swollen rivers and widespread flooding that swamped agricultural land, caused loss of life, and forced tens of thousands of people to evacuate their homes. The event came only a year after the catastrophic floods in Queensland, when the largest part of the north-eastern state was declared a disaster zone. In the aftermath of two major floods in consecutive years, the question arises whether the odds of heavy rain in eastern Australia are set to increase under the synergy between internal climate variability and externally forced climate change. Here we investigate the possible contributions of the ENSO and the long-term effect of human influences on the climate to the heavy rainfall in March 2012 over eastern Australia (10°S–45°S, 140°E–160°E). The anthropogenic contribution is estimated with a new state-of-the-art system for Attribution of extreme weather and Climate Events (ACE; Christidis et al. 2013), built on HadGEM3-A, the latest atmospheric model from the Hadley Centre. We concentrate on March, as the main flooding occurred in the beginning of that month and the total rainfall in the region was exceptionally high in comparison with the summer months (Fig. 19.1a). In fact, March 2012 ranks as the third wettest after 2011 and 1956 in the Global Historical Climatology Network (GHCN) dataset used to provide rainfall observations for this study (Peterson and Vose 1997). Although the heavy rainfall event examined here is not unprecedented, the adverse impacts associated with two consecutive wet years in the region make it an interesting case to study.

The influence of ENSO. A correlation between the phase of ENSO and rainfall in Australia has long been identified (McBride and Nicholls 1983). La Niña episodes, characterized by warm SST anomalies over the West Pacific are associated with wetter-than-normal conditions over eastern Australia. While La Niña conditions prevailed at the end of 2011 and beginning of 2012, they had considerably weakened by March, and ENSO changed phase in April. Figure 19.1b illustrates the relationship between March precipitation in the region and the Southern Oscillation Index (SOI) from summer to early autumn. An increase in rainfall with the SOI is evident, and the slope of the least-square fit is found to be significantly different